Geoid
Journal of Geodesy and Geomatics

Geoid Vol. 21, No. 1, 2026, 38-46

P-ISSN: 1858-2281; E-ISSN: 2442-3998

Analysis of Seasonal Patterns of Atmospheric Water Vapour and Rainfall in East Kalimantan and North Kalimantan Using the Lomb–Scargle Periodogram Method

Agus Ariyanto[1], Eko Yuli Handoko*[2], Putra Maulida[2]
[1] Meteorology Climatology and Geophysics Agency, Indonesia
[2] Department of Geomatics Engineering, Institut Teknologi Sepuluh Nopember Surabaya, Indonesia
*Corresponding author: ekoyh@geodey.its.ac.id

Received: 21 November 2025; Revised: 17 December 2025; Accepted: 18 December 2025; Published: 5 January 2026

Abstract: This study examines the seasonal trends of Precipitable Water Vapour (PWV) obtained from GNSS data (2021–2023) and decadal rainfall data from BMKG (2001–2020) in East and North Kalimantan, employing the Lomb–Scargle Periodogram (LSP) method. The findings indicate that PWV is mostly influenced by an equatorial semi-annual cycle (about 0.5 years), while precipitation typically adheres to a monsoonal annual pattern (around 1 year). The correlation between PWV and precipitation is not wholly linear, exhibiting significant local variability in coastal areas. The LSP approach is effective in identifying dominant frequencies, albeit it exhibits reduced sensitivity to non-stationary fluctuations in atmospheric signals.

Keywords : GNSS, LSP, PWV, Rainfall, Seasonal Pattern

How to cite: Ariyanto, A., Handoko, E. Y., & Maulida, P. (2025). Analysis of seasonal patterns of atmospheric water vapour and rainfall in East Kalimantan and North Kalimantan using the Lomb–Scargle periodogram method. *Geoid, 21*(1), 38-46.

Introduction

Precipitation is an essential component of Earth's climate, dispersing energy and propelling the hydrological cycle that connects the atmosphere, oceans, and terrestrial surfaces (Trenberth et al., 2009). In tropical regions, precipitation exhibits specific patterns shaped by atmospheric and oceanic interactions, with phenomena such as monsoons, intra-seasonal oscillations, and global events like the El Niño–Southern Oscillation (ENSO) and Madden–Julian Oscillation (MJO) significantly influencing these patterns (Chang et al., 2005). Comprehending the formation and transformation of atmospheric water vapour is essential for elucidating tropical weather and climate dynamics.

A valuable tool for studying atmospheric moisture is Precipitable Water Vapour (PWV), which measures the total water vapour in a column of air from the surface to the top of the atmosphere (Kelsey et al., 2022). Over the past two decades, improvements in Global Navigation Satellite System (GNSS) technology have enhanced PWV monitoring, offering greater accuracy and continuous data (Adhi Dermawan et al., 2023; Handoko et al., 2021). This approach relies on analysing the signal delay caused by tropospheric refraction particularly the Zenith Wet Delay (ZWD) component which can be transformed into PWV estimates (Masykur et al., 2021; Vaquero-Martínez & Antón, 2021). Unlike traditional methods such as radiosonde or satellite imagery, GNSS-based estimation can operate under all weather conditions and provide high-frequency data, making it an effective complement for atmospheric water vapour monitoring (Guo et al., 2018; Ning et al., 2016; Rocken et al., 1993).

Atmospheric dynamics in Indonesia, especially in Kalimantan, are influenced by the Asian-Australian monsoon, the Intertropical Convergence Zone (ITCZ), and adjacent bodies of water such as the Sulawesi and Java Seas (Aldrian & Dwi Susanto, 2003). North and East Kalimantan demonstrate significant spatial and temporal variability in rainfall patterns, with wet and dry periods that do not consistently align with the traditional monsoonal calendar (Maulida et al., 2025). Analyzing the periodic behavior of PWV can provide

insights into the seasonal and intra-seasonal climate patterns of the region (Baldysz et al., 2021).

This research examines the seasonal patterns and variability of PWV utilizing GNSS data from 2021 to 2023, while also analyzing its relationship with decadal rainfall data from BMKG (2001–2020) in North and East Kalimantan. The research employs Lomb–Scargle spectral analysis to identify dominant cycles in atmospheric water vapor and elucidate the relationship between PWV variability and rainfall patterns in these regions.

Methodology

Study Area and Data

This study utilizes two primary datasets: PWV derived from GNSS observations and conventional rainfall observation data. The GNSS data were obtained from the Continuously Operating Reference Station (CORS) network managed by the Geospatial Information Agency of Indonesia (BIG) for the period 2021–2023. Meanwhile, rainfall data were provided by the Meteorological, Climatological, and Geophysical Agency (BMKG) covering the observation period from 2001 to 2020, with a temporal resolution of ten days (decadal). These data were used to characterize the long-term seasonal patterns and rainfall variability across the study region.

The research area includes six representative stations across Kalimantan Island, comprising three locations in North Kalimantan (Bulungan, Nunukan, and Tarakan) and three in East Kalimantan (Samarinda, Berau, and Balikpapan). The selection of these sites was based on both geographical and climatological considerations to capture the contrasting characteristics between coastal and inland regions in the northern and eastern parts of Kalimantan **(Figure 1)**.

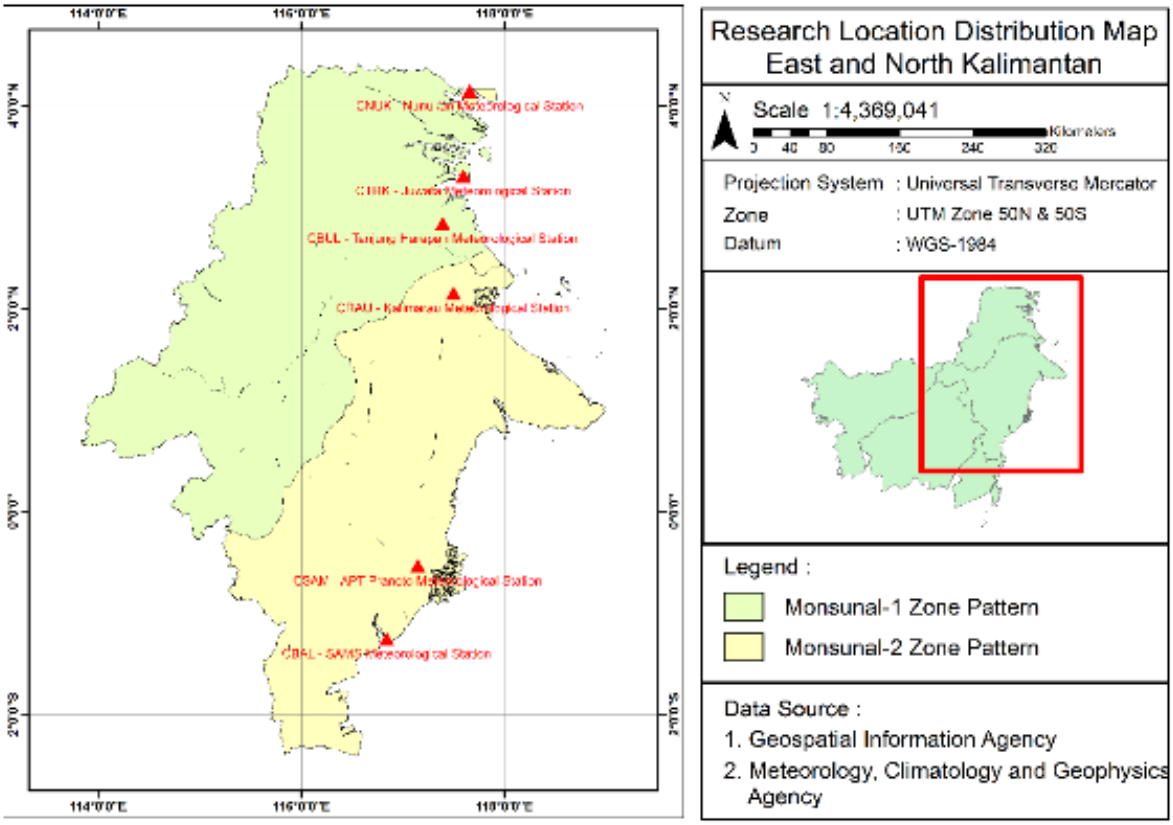

Figure 1 Research Location MAP, CORS and Meteorology Station

Table 1 CORS and Meteorology Station

Location	CORS	Meteorology Station Name
Samarinda	CSAM	APT Pranoto
Berau	CRAU	Kalimarau
Balikpapan	CBAL	SAMS
Bulungan	CBUL	Tanjung Harapan
Nunukan	CNUK	Nunukan
Tarakan	CTRK	Juwata

PWV Data Processing

The evolution of GNSS signal processing for ZWD estimate has been marked by the advancement of the Precise Point Positioning (PPP) technique (Geng et al., 2019, 2023; Hankansujarit & Andrei, 2018; Mikoś et al., 2023). This procedure is facilitated by open-source software, including PRIDE-PPPAR, which employs the ztd Piecewise Constant (PWC) approximation model with Vienna Mapping Function corrections (Li et al., 2023; Yang et al., 2020). These innovations can improve the accuracy of ZTD and ZWD estimates, including under complex tropical atmospheric conditions (Landskron & Böhm, 2018; Maulida et al., 2020). ZWD was converted to PWV using the Bevis formula (Bevis et al., 1992) :

$$PWV = \pi . ZWD \tag{1}$$

where

$$\pi = \frac{10^6}{\rho_w R_v \left(\frac{k_3}{T_m} + k_2'\right)} \tag{2}$$

With PWV and ZWD in (mm), $k_2' = 22.1\ K/hPa$ and $k_3 = 373900\, K^2/hPa$ is as empirical refractivity constants, T_m represents the weighted mean atmospheric temperature in Kelvin (K), $\rho_w = 1000\ kg/m^3$ is the density of liquid water, and $R_v = 461.495\ J/kgK$ is the specific gas constant for water vapor.

Periodicity Analysis

This study utilizes the Lomb–Scargle Periodogram (LSP) approach to discern the seasonal patterns and predominant frequencies of PWV changes. The LSP was initially created by William H. Lomb in 1976 and subsequently enhanced by Jeffrey Richard Scargle in 1983 as a method of spectral analysis tailored for time series data with variable observation intervals (Lomb, 1976; Scargle, 1983). LSP is a variant of the Discrete Fourier Transform (DFT) that calculates the energy distribution of a signal in the frequency domain to derive the power spectral density (PSD) (VanderPlas, 2018). This approach is adept at identifying periodic components in PWV signals, even within temporal abnormalities frequently observed in GNSS-derived data.

This study began with the creation of PWV time series from each observation station, followed by data normalisation to eliminate long-term trends that could affect spectral stability. The Lomb–Scargle spectrum was then calculated to detect power peaks indicating dominant frequencies. These frequencies were then converted into periods (measured in years or months) and analysed for annual (monsoonal), semi-annual (equatorial), and intra-seasonal (local) oscillation patterns. Monsoon patterns were identified when the dominant period was in the range of 0.83–1.17 years. Equatorial patterns are defined for periods of 0.42–0.58 years, corresponding to the characteristics of two annual rainfall peaks in the equatorial zone. Local patterns are categorised within the period range of 0.25–0.375 years, which are generally associated with short-scale atmospheric variability and orographic effects. Periods outside these three ranges are classified as ‘other’, which includes non-seasonal variability such as the MJO, inter-seasonal signals, or noise. This study

emphasises that these period ranges form an 'operational window' or frequency tolerance specifically defined for spectral analysis-based classification purposes. This method provides a quantitative representation of atmospheric water vapour dynamics and facilitates the identification of characteristic periodicities associated with rainfall patterns and climate variability in tropical maritime zones.

The difference in time ranges in the data used does not reduce the validity of the frequency analysis, but it needs to be explicitly stated as a limitation of the study. In climatology, long-term rainfall patterns (≥ 10 years) are used to describe the seasonal characteristics of a region. Since PWV is an atmospheric variable that is strongly influenced by the monsoon cycle and equatorial dynamics, its periodic patterns can be compared with general rainfall patterns without having to be in the same year range. Thus, rainfall over 20 years (2001-2020) is used to obtain representative climatological patterns, while 3 years of PWV (2021-2023) is sufficient to detect dominant frequencies through LSP.

Results and Discussion

Results of LSP Analysis on PWV

At each location, the highest peak in the Lomb–Scargle periodogram indicates the primary characteristic of atmospheric water vapor dynamics. In Samarinda **(Figure 2.a)**, the primary peak is observed at a period of 0.53 years (6.4 months), signifying the impact of equatorial patterns characterized by a semi-annual cycle. In Berau **(Figure 2.b)**, the dominant period of 0.51 years (6.2 months) indicates a consistent equatorial signal. In contrast, Balikpapan **(Figure 2.c)** demonstrates a dominant period of 1.12 years (13.5 months), indicating the presence of an annual seasonal cycle influenced by monsoonal factors.

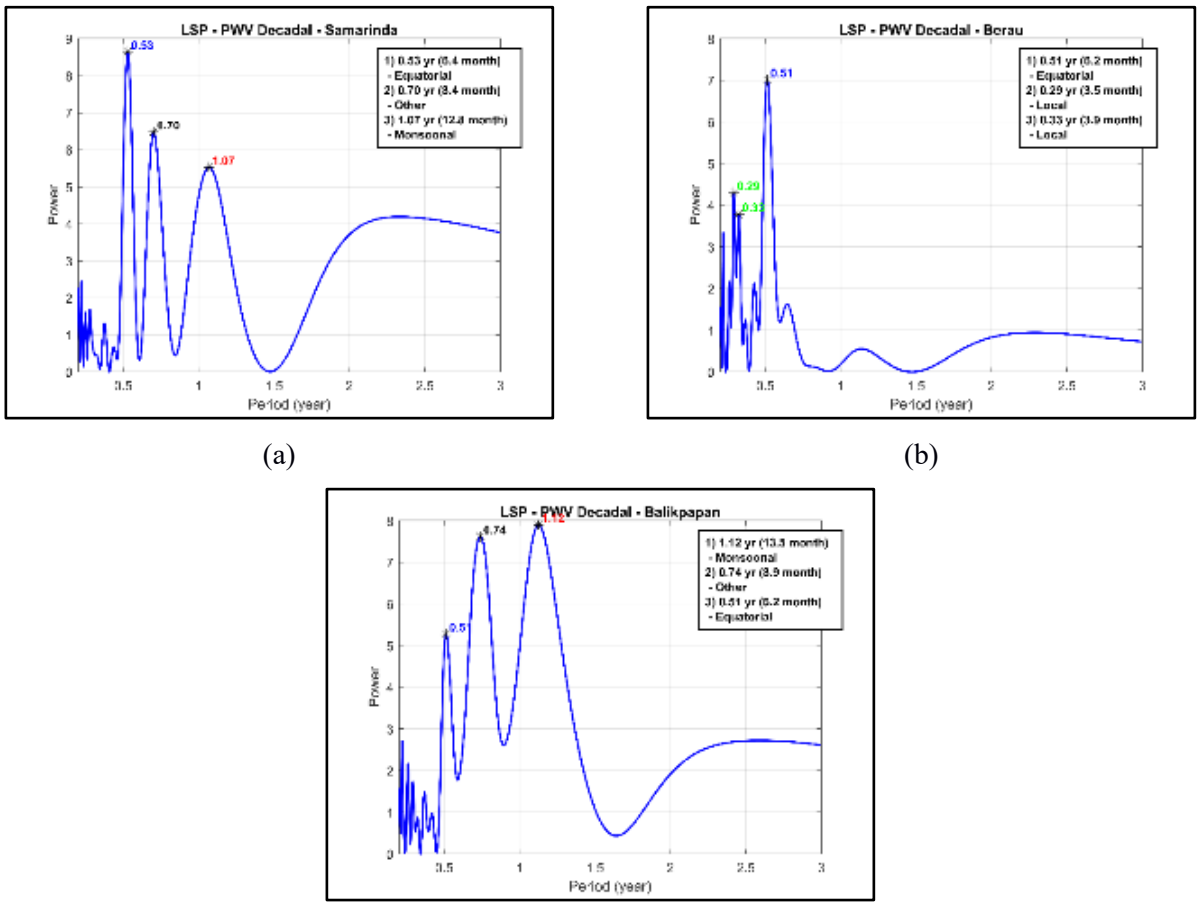

(a) (b)

(c)

Figure 2 Lomb–Scargle Periodogram of PWV Patterns in East Kalimantan Province: (a) Samarinda, (b) Berau, and (c) Balikpapan

In addition to these primary peaks, each site also displays several secondary periodic components. Samarinda and Balikpapan show both annual and intermediate-scale variations, while Berau reveals localized oscillations on a 3–4 month timescale. In Bulungan and Nunukan **(Figure 3.a and 3.b)**, the Lomb–Scargle periodogram reveals dominant peaks at 0.53 years (6.3 months) and 0.54 years (6.5 months), reflecting the influence of semi-annual equatorial cycles on atmospheric water vapor dynamics. In contrast, Tarakan **(Figure 3.c)** shows a distinct peak at 0.29 years (3.5 months), indicating a stronger local modulation, followed by a secondary peak at 0.22 years (2.7 months). While the equatorial signal at 0.52 years (6.2 months) remains evident in Tarakan, the results suggest that local atmospheric processes exert a greater impact there than in Bulungan and Nunukan.

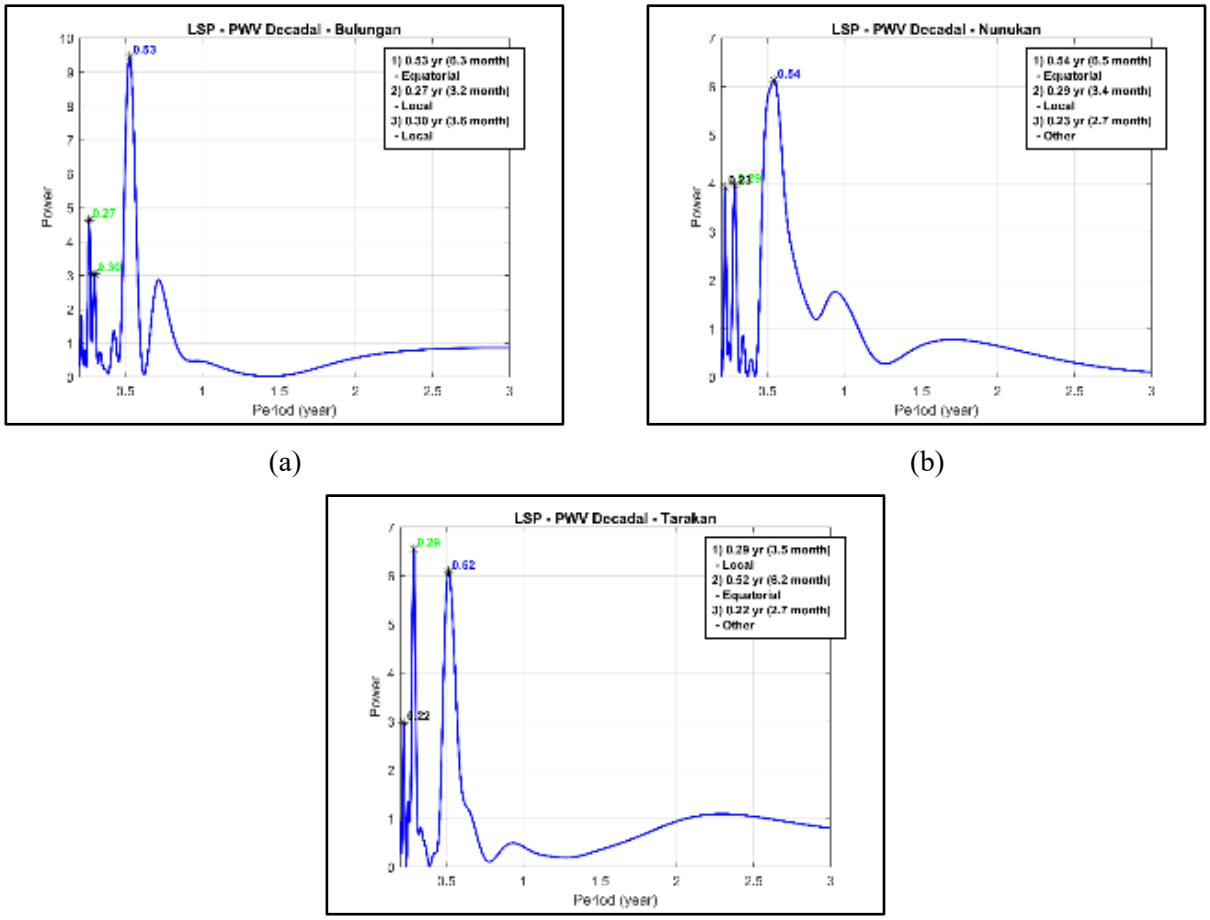

Figure 3 Lomb–Scargle Periodogram of PWV Patterns in North Kalimantan Province: (a) Bulungan, (b) Nunukan, and (c) Tarakan

The analysis of PWV data from East Kalimantan (Samarinda, Berau, and Balikpapan) and North Kalimantan (Bulungan, Nunukan, and Tarakan) using the Lomb–Scargle periodogram indicates a consistent periodic pattern. This pattern is primarily influenced by the equatorial semi-annual cycle, which has a duration of approximately 0.5 years. Most observation sites display prominent peaks within the range of 0.51 to 0.54 years (6–6.5 months), indicating the significant equatorial influences that regulate atmospheric water vapour dynamics in the area. Annual peaks, occurring approximately once a year, are observed in Balikpapan and Samarinda, indicating the impact of the monsoonal cycle. Stations such as Bulungan, Nunukan, and Tarakan exhibit more pronounced local variability components at shorter periods, specifically in the range of approximately 0.2 to 0.3 years. The spatial distribution of PWV periodicity across both provinces exhibits a distinct gradient. East Kalimantan demonstrates a greater influence from monsoonal activity, while North Kalimantan is primarily affected by equatorial variability.

Results of LSP Analysis on Rainfall

The Lomb–Scargle periodogram analysis of decadal rainfall data in Samarinda, Berau, and Balikpapan indicates that all three regions in East Kalimantan are primarily characterized by annual periods (approximately 1.00–1.09 years). This finding suggests a monsoonal rainfall pattern with a stable seasonal cycle. In Samarinda and Berau **(Figure 4.a and 4.b)**, secondary periods ranging from 0.50 to 0.54 years indicate the existence of an equatorial-type rainfall regime, characterized by two distinct rainfall peaks annually. In contrast, Balikpapan **(Figure 4.c)** demonstrates a pronounced annual pattern, characterized by multiple closely spaced annual components that indicate the ongoing influence of monsoonal conditions throughout the year.

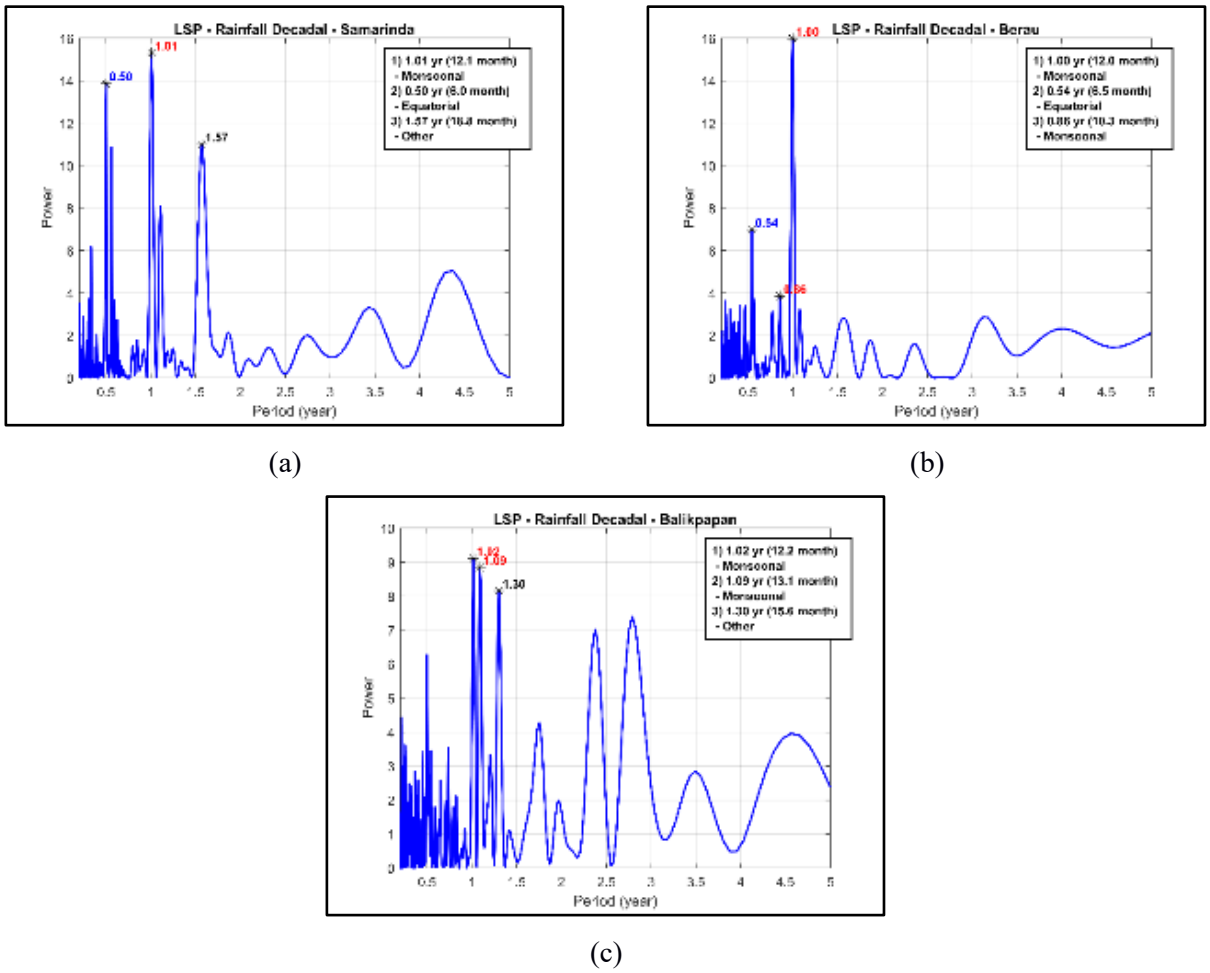

Figure 4 Lomb–Scargle Periodogram of Rainfall Patterns in East Kalimantan Province: (a) Samarinda, (b) Berau, and (c) Balikpapan

The Lomb–Scargle periodogram analysis of decadal rainfall data in North Kalimantan reveals distinct periodic characteristics across different locations. In Bulungan **(Figure 5.a)**, two dominant peaks at 0.99 years (11.9 months) and 1.06 years (12.7 months) indicate a monsoonal rainfall pattern, characterized by a single major wet season within the annual cycle, along with a local variability component around 0.28 years (3.3 months) likely associated with short-term climatic fluctuations. In Nunukan **(Figure 5.b)**, the dominant annual peak at 1.00 year (12.0 months) reflects a strong monsoonal signal, while the secondary period of 2.20 years (26.4 months) suggests the presence of an interannual cycle, and the 0.57-year (6.8 months) period represents an equatorial rainfall pattern with two peaks per year. Meanwhile, in Tarakan **(Figure 5.c)**, the rainfall regime is primarily governed by equatorial dynamics, as indicated by two major peaks at 0.50 years (6.0 months) and 0.52 years (6.2 months), with additional local variability observed at a shorter period of around 0.36 years (4.4 months).

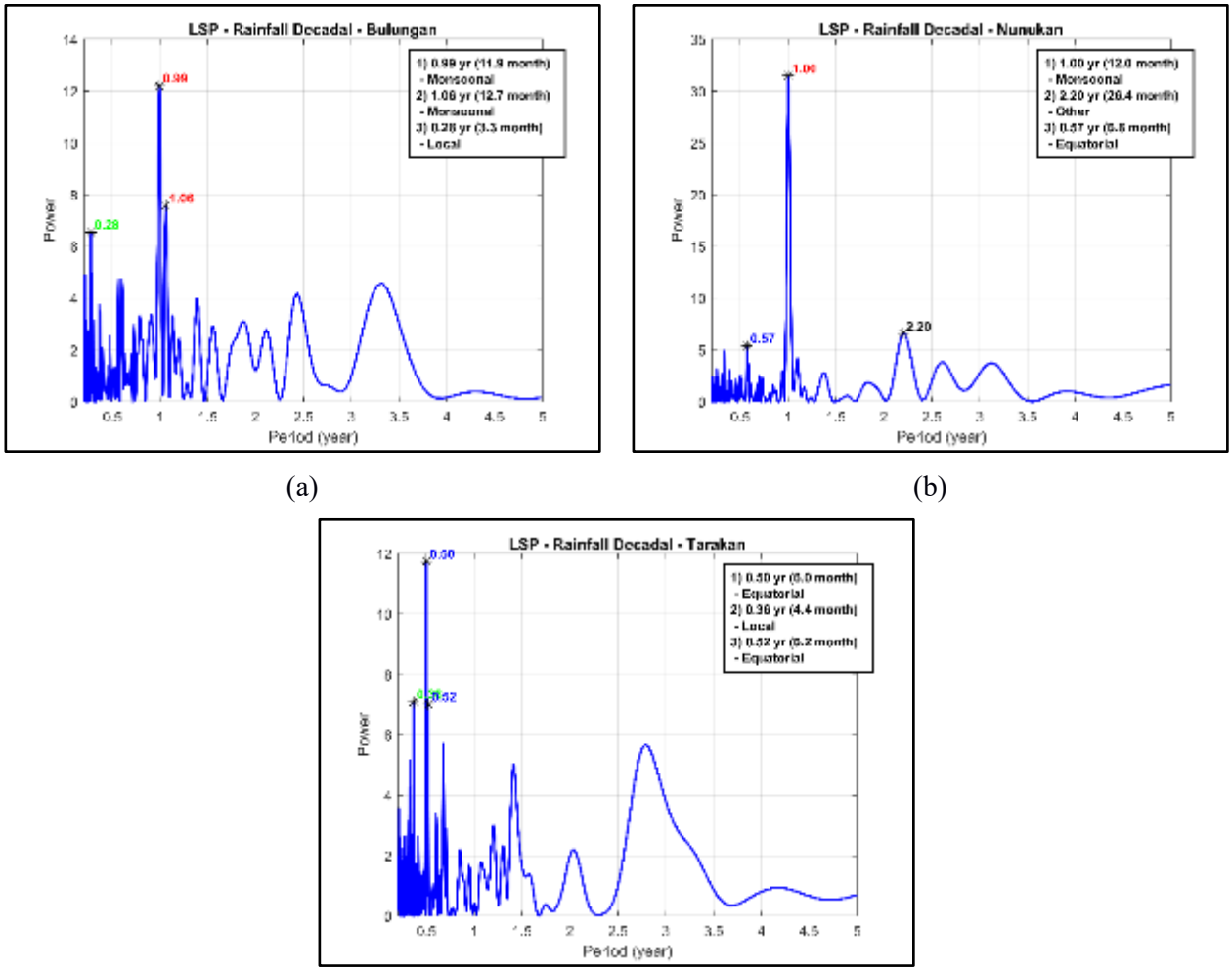

(a) (b)

(c)

Figure 5 Lomb–Scargle Periodogram of Rainfall Patterns in North Kalimantan Province: (a) Bulungan, (b) Nunukan, and (c) Tarakan

Table 2. The Comparison of LSP Peak Periods between PWV and Rainfall

Location	PWV	Pattern PWV	Rainfall	Pattern Rainfall
Samarinda	0.53	Equatorial	1.01	Monsoonal
Berau	0.51	Equatorial	1.00	Monsoonal
Balikpapan	1.12	Monsoonal	1.02	Monsoonal
Bulungan	0.53	Equatorial	0.99	Monsoonal
Nunukan	0.54	Equatorial	1.00	Monsoonal
Tarakan	0.29	Local	0.50	Equatorial

The comparative analysis of patterns **(Table 2)** reveals that the spatial relationship between PWV and rainfall across northern and eastern Kalimantan is complex and not entirely linear. In Balikpapan, both PWV and rainfall display monsoonal traits, highlighting a significant connection between atmospheric water vapor dynamics and seasonal precipitation systems. In contrast, Tarakan reveals an intriguing anomaly, where PWV exhibits localized variability, while rainfall follows an equatorial-type pattern. This difference indicates that

precipitation processes in small coastal regions such as Tarakan are mainly influenced by local convection and maritime effects, rather than by broader regional water vapor variability.

Meanwhile, in Samarinda, Berau, Bulungan, and Nunukan, although PWV tends to follow an equatorial pattern, rainfall is more monsoonal in nature. This indicates that rainfall distribution in these regions is largely controlled by monsoonal circulation systems and large-scale air mass movements, rather than by local fluctuations in atmospheric moisture. Overall, these findings emphasize that the PWV precipitation relationship is not necessarily direct, but rather mediated by multiscale atmospheric dynamics that modulate moisture transport and rainfall formation across the region.

Conclusions

The Lomb–Scargle Periodogram analysis indicates that most study areas Samarinda, Berau, Bulungan, and Nunukan exhibit a dominant semi-annual pattern (approximately 0.5 years), reflecting an equatorial climatic character, whereas Balikpapan shows a strong annual cycle (~1 year) influenced primarily by monsoonal dynamics. In contrast, Tarakan displays a shorter periodicity (~0.3 years), suggesting the predominance of localized convective processes.

Comparison with rainfall patterns reveals that the relationship between PWV and precipitation is nonlinear. Regions such as Balikpapan, where PWV exhibits a monsoonal pattern, show a close alignment with seasonal rainfall cycles, while in Tarakan, discrepancies arise due to the dominance of local convection. Overall, the variability of PWV and rainfall across Kalimantan is governed by multiscale atmospheric interactions, involving the monsoon system, equatorial oscillations, and local-scale processes.

The Lomb–Scargle Periodogram proves to be an effective method for detecting periodic patterns and dominant frequencies in PWV data with uneven temporal sampling. Its main advantage lies in its ability to analyze irregular time series without interpolation. However, it is less effective in capturing non-stationary or short-term frequency variations, suggesting that combining LSP with time–frequency methods such as the Wavelet Transform would provide a more comprehensive understanding of tropical atmospheric dynamics.

Acknowledgment

The authors express gratitude to the Geospatial Information Agency (BIG) as a data provider and the Meteorology, Climatology and Geophysics Agency (BMKG) as a funder.

References

Adhi Dermawan, A. A., Handoko, E. Y., & Maulida, P. (2023). An Estimation of Precipitable Water Vapour Around Surabaya City Using GIPSY-X. *IOP Conference Series: Earth and Environmental Science*, *1127*(1), 12004. https://doi.org/10.1088/1755-1315/1127/1/012004

Aldrian, E., & Dwi Susanto, R. (2003). Identification of three dominant rainfall regions within Indonesia and their relationship to sea surface temperature. *International Journal of Climatology*, *23*(12), 1435–1452. https://doi.org/https://doi.org/10.1002/joc.950

Baldysz, Z., Nykiel, G., Latos, B., Baranowski, D. B., & Figurski, M. (2021). Interannual Variability of the GNSS Precipitable Water Vapor in the Global Tropics. In *Atmosphere* (Vol. 12, Issue 12). https://doi.org/10.3390/atmos12121698

Bevis, M., Businger, S., Herring, T. A., Rocken, C., Anthes, R. A., & Ware, R. H. (1992). GPS meteorology: remote sensing of atmospheric water vapor using the global positioning system. *Journal of Geophysical Research*, *97*(D14). https://doi.org/10.1029/92jd01517

Chang, C.-P., Wang, Z., McBride, J., & Liu, C.-H. (2005). Annual Cycle of Southeast Asia—Maritime Continent Rainfall and the Asymmetric Monsoon Transition. *Journal of Climate*, *18*(2), 287–301. https://doi.org/10.1175/JCLI-3257.1

Geng, J., Chen, X., Pan, Y., Mao, S., Li, C., Zhou, J., & Zhang, K. (2019). PRIDE PPP-AR: an open-source software for GPS PPP ambiguity resolution. *GPS Solutions*, *23*. https://doi.org/10.1007/s10291-019-0888-1

Geng, J., Ge, M., Yang, S., Zhang, K., Lin, J., Li, W., Mao, S., Pan, Y., & Zeng, J. (2023). *PPP-AR III Manual*. Wuhan

University. https://pride.whu.edu.cn/ueditor/jsp/upload/file/20231124/1700793919577054879.pdf

Guo, Q., Wu, X., & Sang, W. (2018). *Review of the Research Status and Progress of Ground-Based GNSS Meteorology*. *Iweg*, 199–206. https://doi.org/10.5220/0007428101990206

Handoko, E. Y., Kurniawan, A., Maulida, P., & Cemara, N. A. (2021). Precipitation Water Vapour Variation in the East Java Region from Data CORS Using GIPSY. *IOP Conference Series: Earth and Environmental Science*, *936*(1), 12001. https://doi.org/10.1088/1755-1315/936/1/012001

Hankansujarit, C., & Andrei, C. O. (2018). Atmospheric water estimation using GNSS precise point positioning method. *Engineering Journal*, *22*(6), 37–45. https://doi.org/10.4186/ej.2018.22.6.37

Kelsey, V., Riley, S., & Minschwaner, K. (2022). Atmospheric precipitable water vapor and its correlation with clear-sky infrared temperature observations. *Atmospheric Measurement Techniques*, *15*(5), 1563–1576. https://doi.org/10.5194/amt-15-1563-2022

Landskron, D., & Böhm, J. (2018). VMF3/GPT3: refined discrete and empirical troposphere mapping functions. *Journal of Geodesy*, *92*(4), 349–360. https://doi.org/10.1007/s00190-017-1066-2

Li, F., Li, J., Liu, L., Huang, L., Zhou, L., & He, H. (2023). Machine Learning-Based Calibrated Model for Forecast Vienna Mapping Function 3 Zenith Wet Delay. In *Remote Sensing* (Vol. 15, Issue 19). https://doi.org/10.3390/rs15194824

Lomb, N. R. (1976). Least-squares frequency analysis of unequally spaced data. *Astrophysics and Space Science*, *39*(2), 447–462. https://doi.org/10.1007/BF00648343

Masykur, M., Handoko, E. Y., & Susilo. (2021). Web-Based Online Post-Processing GNSS Service InaCORS BIG for Mapping Control Point Positioning for Channel or Road Design. *IOP Conference Series: Earth and Environmental Science*, *936*(1), 12024. https://doi.org/10.1088/1755-1315/936/1/012024

Maulida, N. P., Ariska, M., Suhadi, S., & Akhsan, H. (2025). Rainfall Characteristics in Kalimantan Island During ENSO and IOD Phases: Insights from Composite Analysis. *JURNAL ILMU FISIKA | UNIVERSITAS ANDALAS*, *17*(1 SE-Research Article), 88–100. https://doi.org/10.25077/jif.17.1.88-100.2025

Maulida, N. P., Landskron, D., & Böhm, J. (2020). Assessing the performance of Vienna Mapping Functions 3 for GNSS stations in Indonesia using Precise Point Positioning. *Adv. Geosci.*, *50*, 77–86. https://doi.org/10.5194/adgeo-50-77-2020

Mikoś, M., Kazmierski, K., Hadas, T., & Sośnica, K. (2023). Multi-GNSS PPP solutions with different handling of system-specific receiver clock parameters and inter-system biases. *GPS Solutions*, *27*(3), 137. https://doi.org/10.1007/s10291-023-01474-w

Ning, T., Wang, J., Elgered, G., Dick, G., Wickert, J., Bradke, M., Sommer, M., Querel, R., & Smale, D. (2016). The uncertainty of the atmospheric integrated water vapour estimated from GNSS observations. *Atmospheric Measurement Techniques*, *9*(1), 79–92. https://doi.org/10.5194/amt-9-79-2016

Rocken, C., Ware, R., Van Hove, T., Solheim, F., Alber, C., Johnson, J., Bevis, M., & Businger, S. (1993). Sensing atmospheric water vapor with the global positioning system. *Geophysical Research Letters*, *20*(23), 2631–2634. https://doi.org/10.1029/93GL02935

Scargle, J. (1983). Studies in astronomical time series analysis. II - Statistical aspects of spectral analysis of unevenly spaced data. *The Astrophysical Journal*, *263*. https://doi.org/10.1086/160554

Trenberth, K. E., Fasullo, J. T., & Kiehl, J. (2009). Earth's Global Energy Budget. *Bulletin of the American Meteorological Society*, *90*(3), 311–324. https://doi.org/10.1175/2008BAMS2634.1

VanderPlas, J. T. (2018). Understanding the Lomb–Scargle Periodogram. *The Astrophysical Journal Supplement Series*, *236*(1), 16. https://doi.org/10.3847/1538-4365/aab766

Vaquero-Martínez, J., & Antón, M. (2021). Review on the Role of GNSS Meteorology in Monitoring Water Vapor for Atmospheric Physics. In *Remote Sensing* (Vol. 13, Issue 12). https://doi.org/10.3390/rs13122287

Yang, L., Gao, J., Zhu, D., Zheng, N., & Li, Z. (2020). Improved Zenith Tropospheric Delay Modeling Using the Piecewise Model of Atmospheric Refractivity. In *Remote Sensing* (Vol. 12, Issue 23). https://doi.org/10.3390/rs12233876